Shear wave velocity structure from high resolution 2-D Rayleigh wave group velocity tomography for India and surrounding regions.

Siddharth Dey[1] and Supriyo Mitra[1]

[1]IISER Kolkata

November 24, 2022

Abstract

We use 7823 regional waveforms from 2520 earthquakes (M > 4.0) recorded at 244 stations, located on the Indian subcontinent and Tibet, to compute fundamental mode Rayleigh wave group velocity dispersion curves between 10 s and 120 s. The Rayleigh waveforms for all these traces had a signal-to-noise ratio above two for the periods of our interest. The dataset provides a dense sampling of the Bay of Bengal and the Arabian Sea, the Indian subcontinent, the Himalayan foreland basin, the Himalaya, and the Tibetan Plateau, between latitudes -8° to 40° and longitudes 60° to 100°. These 1-D path average group velocity curves were linearly combined through a ray theory based tomography formulation to obtain 2-D maps of lateral variation of group velocities at discrete periods. For the tomography the region is parametrised as 1° triangular elements with slowness defined at the apex of each triangle (node points). The coverage and resolution of the tomography maps are explored by computing ray density map, raypath orientation map and a standard checker board resolution test. The best resolved features in the tomography maps are at periods between 15 s and 45 s and is of the order of 4° x 4°. From the ray density and raypath orientation maps we observe that the best resolved grids are the ones where there is maximum ray density and uniform raypath orientation. To optimise the choice of the apriori slowness vis-a-vis the sharpness of the observed anomalies in the tomography inversion, we performed apriori slowness test. We used a number of fixed apriori slowness values and computed the tomography images for every period. A plot of the apriori slowness versus sum of squares(residuals) provides the choice for the optimum value for every period. We observe that for most periods this is marked by a minimum in the tradeoff curve. The regions with low velocities depict the basin areas with high sediment cover whereas the high velocity regions are indicative of the cratons and shield areas. Finally, we model the group velocity curve at each node point using a quasi-linear least squares inversion scheme of Ammon and Hermann (2004) to obtain 1-D shear wave velocity structure beneath the node point. We will use cubic spline interpolation through these 1-D models to obtain 3-D shear wave velocity structure across the region of interest.

Shear wave velocity structure from high resolution 2-D Rayleigh wave group velocity tomography for India and surrounding regions.

Siddharth Dey and Supriyo Mitra

sd13ip033@iiserkol.ac.in

Department of Earth Sciences, Indian Institute of Science Education and Research Kolkata, West Bengal, India

EGU 2019 - 458

Abstract

We use 7823 regional waveforms from 2520 earthquakes (M > 4.0) recorded at 244 stations, located on the Indian subcontinent and Tibet, to compute fundamental mode Rayleigh wave group velocity dispersion curves between 10 s and 120 s. The Rayleigh waveforms for all these traces had a signal-to-noise ratio above two for the periods of our interest. The dataset provides a dense sampling of the Bay of Bengal and the Arabian Sea, the Indian subcontinent, the Himalayan foreland basin, the Himalaya, and the Tibetan Plateau, between latitudes -8° to 40° and longitudes 60° to 100°. These 1-D path average group velocity curves were linearly combined through a ray theory based tomography formulation to obtain 2-D maps of lateral variation of group velocities at discrete periods. For the tomography the region is parametrised as 1° triangular elements with slowness defined at the apex of each triangle (node points). The coverage and resolution of the tomography maps are explored by computing ray density map, raypath orientation map and a standard checker board resolution test. The best resolved features in the tomography maps are at periods between 15 s and 45 s and is of the order of 4° x 4°. From the ray density and raypath orientation maps we observe that the best resolved grids are the ones where there is maximum ray density and uniform raypath orientation. To optimise the choice of the apriori slowness vis-a-vis the sharpness of the observed anomalies in the tomography inversion, we performed apriori slowness test. We used a number of fixed apriori slowness values and computed the tomography images for every period. A plot of the apriori slowness versus sum of squares(residuals) provides the choice for the optimum value for every period. We observe that for most periods this is marked by a minimum in the tradeoff curve. The regions with low velocities depict the basin areas with high sediment cover whereas the high velocity regions are indicative of the cratons and shield areas. Finally, we model the group velocity curve at each node point using a quasi-linear least squares inversion scheme of Ammon and Hermann (2004) to obtain 1-D shear wave velocity structure beneath the node point. We will use cubic spline interpolation through these 1-D models to obtain 3-D shear wave velocity structure across the region of interest.

Data and Methodology

A total of 2520 events from the ISC reviewed catalogue which are scaled according to their magnitude of occurrence (figure 1a) and a total of 244 stations belonging to both global and Indian sources (figure 1b) , are used for this study. The number of ray paths used for tomography at every discrete period is showed in the histogram (figure 1c).

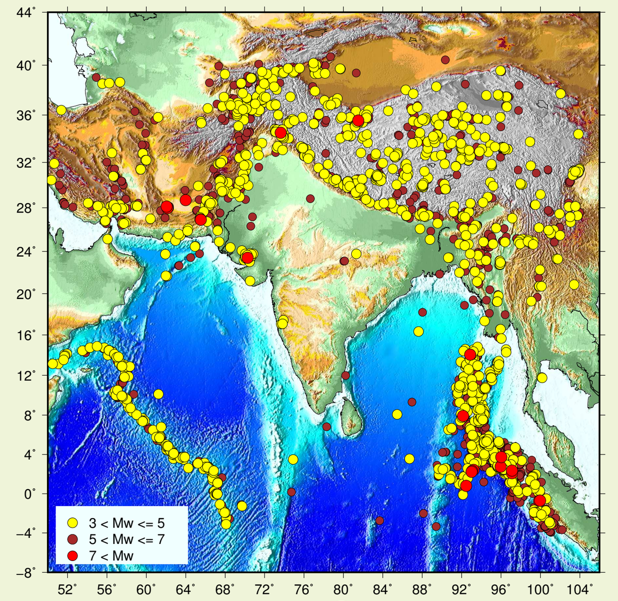

1a

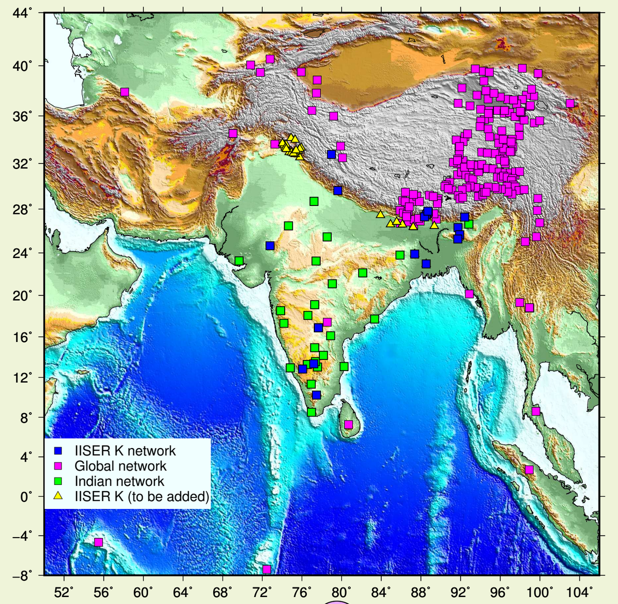

1b

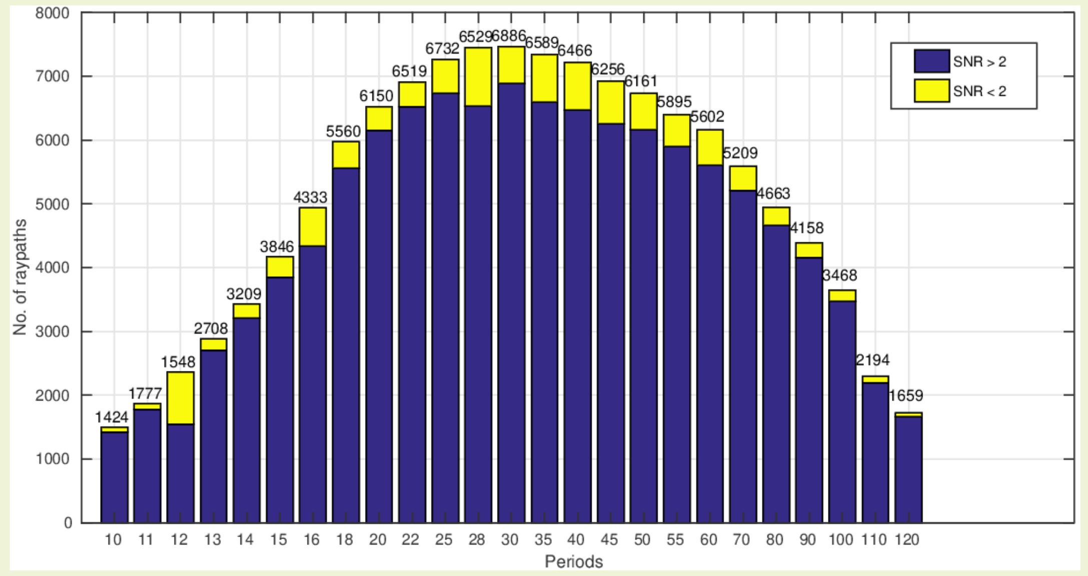

1c

Every trace in vertical component is filtered from 10sec to 150sec to extract the Rayleigh wave packet. Using Hermann's multiple filtering technique, the group velocity dispersion is measured for the fundamental mode part and their estimated errors. Then we combine the group velocity data to produce tomographic group velocity maps of the whole region of India and Tibet. Each node point of the triangular mesh (shown below) is described by a position vector from the centre of the Earth. The group slowness is calculated at the nodes of these triangles from intersecting propagation paths for which group velocity dispersion measurements were made. A three-point linear interpolation was used to evaluate the model within each triangular element in the gridded region.

For an earthquake source receiver ray path, the time taken can be expressed as on the equation on the left :

$$t = \int_{path} u \, dx = \sum_{i=0}^{n} \int_0^{l_i} u \, dx \qquad u = \varepsilon_0 u(\mathbf{x_0}) + \varepsilon_1 u(\mathbf{x_1}) + \varepsilon_2 u(\mathbf{x_2})$$

u is the slowness, li denotes the length of the ray path segment within the ith triangle, and the summation is over all triangles. The x0, x1 and x2 are the position vectors of the triangle node points.
Summing over the node points of the triangles, we get :

$$t = \sum_{points} u(x) \sum_{triangles} \int \varepsilon \, dx \Longrightarrow \mathbf{d} = [\mathrm{G}] \text{ x } \mathbf{m}$$

which is the expression of forward problem, where d is the N-dimensional vector of travel time data t, m is an M-dimensional vector of the slowness values at the nodes, and [G] is the operator that maps vectors in the model space into vectors in the data space. We solve for the model vector m by minimizing the sum of the data-weighted sum of squares and the smoothed sum of squares for the model vector, formulated as

$$\text{data sum of squares} = (\mathrm{d} - \mathrm{Gm})^{\mathrm{T}} \mathrm{V}^{-1} (\mathrm{d} - \mathrm{Gm}) \quad \text{and} \quad \text{smoothed sum of squares} = \mathrm{m}^{\mathrm{T}} \mathrm{V_s}^{-1} \mathrm{m}$$

where V is the data variance matrix and Vs is the variance matrix associated with the apriori probability constraints on the model vector m.

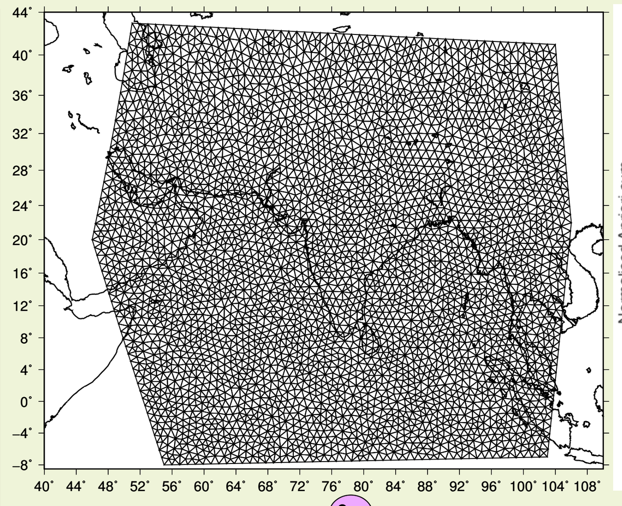

2a

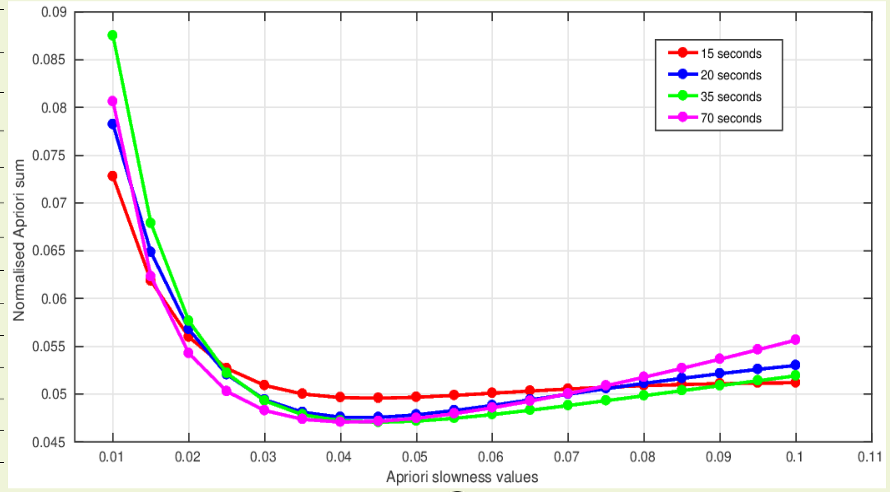

2b

The region of interest is parameterised by a 2D mesh of 1° sided triangles, where the the slowness values are calculated at the node points (figure 2a). Trade-off curves between apriori slowness values and their corresponding apriori sum (normalised) at three different periods (figure 2b). The optimum value indicating a measure between spread of resolution and variance lies in the range of 0.035 and 0.05 for most of the periods in the tomgraphy.

Tests for tomography at 15sec period

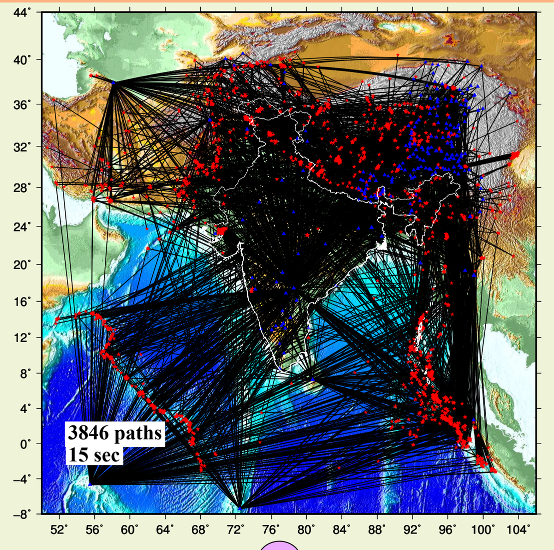

3a

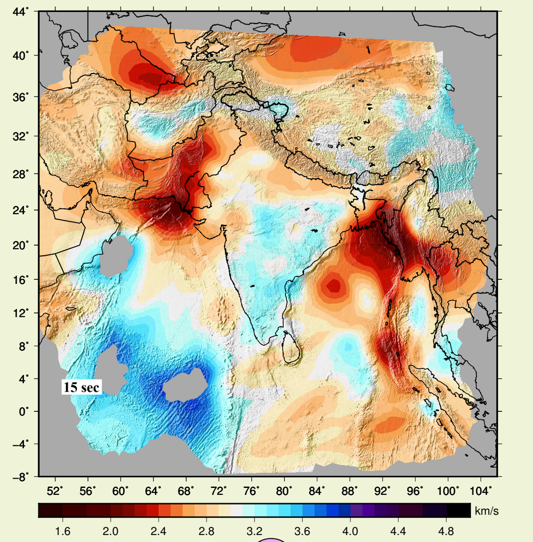

3b

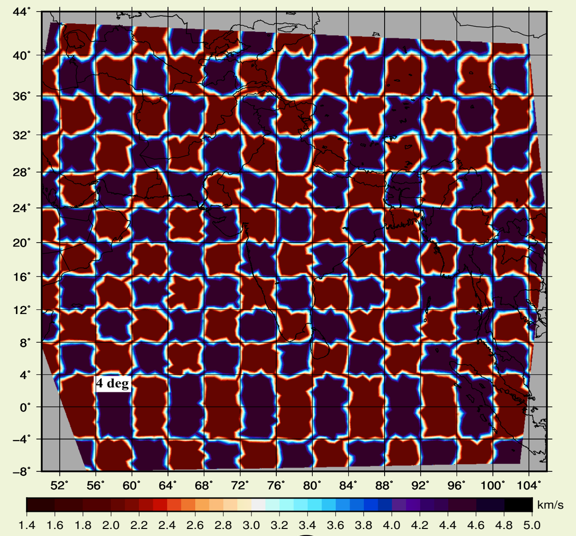

3c

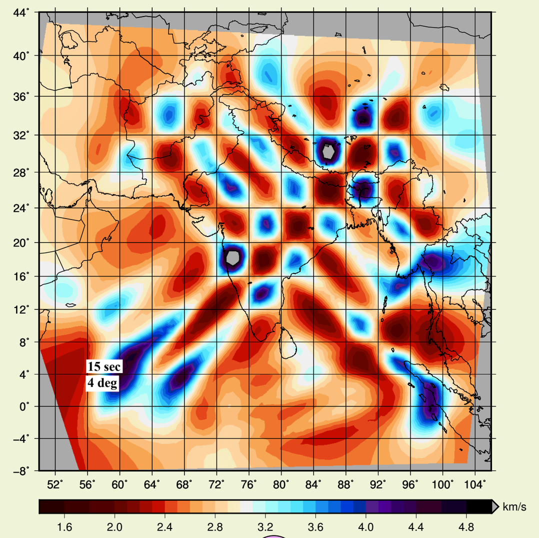

3d

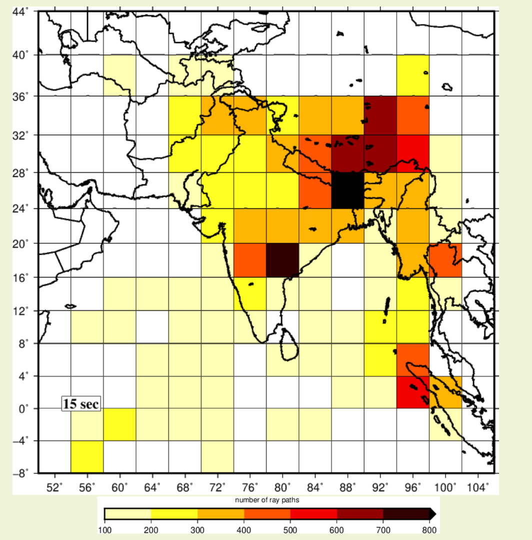

3e

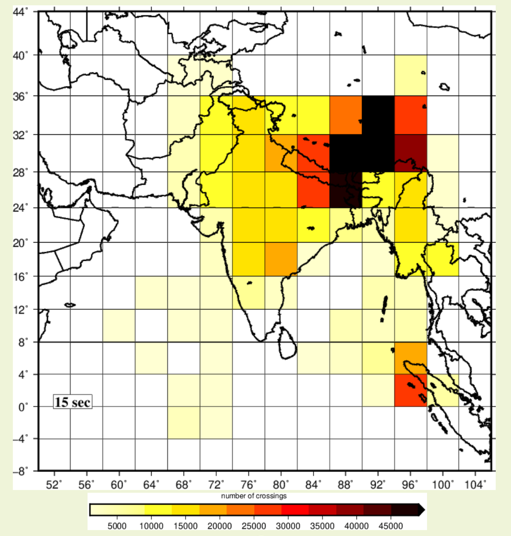

3f

Maps and results of few tests at 15 sec are shown above. Figure 3a is the ray coverage map with 3846 ray paths. Figure 3b is the absolute scale group velocity tomography map. The grey areas represent the velocity values higher than 0.3 km/s. Figure 3c is the checker board input map of 4° grid size with 1.8km/s (lower end) and 4.2km/s (higher end). Figure 3d is the corresponding checker board output result. The grey areas within the blue spots have the output values are higher than the 5km/s. Figure 3e shows the number of ray paths passing through each grid and figure 3f shows the number of ray path intersection in each grid which correlate with better resolved areas in checker board output map.

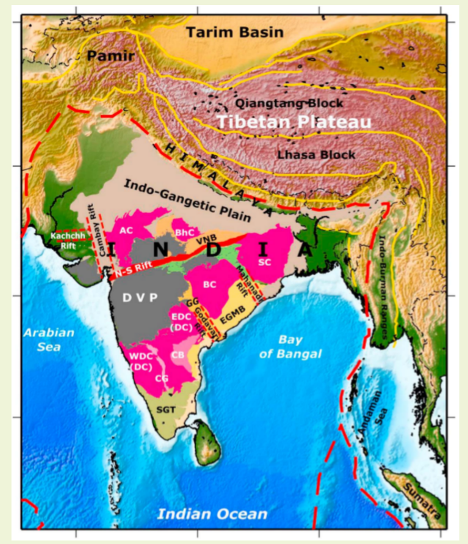

4a

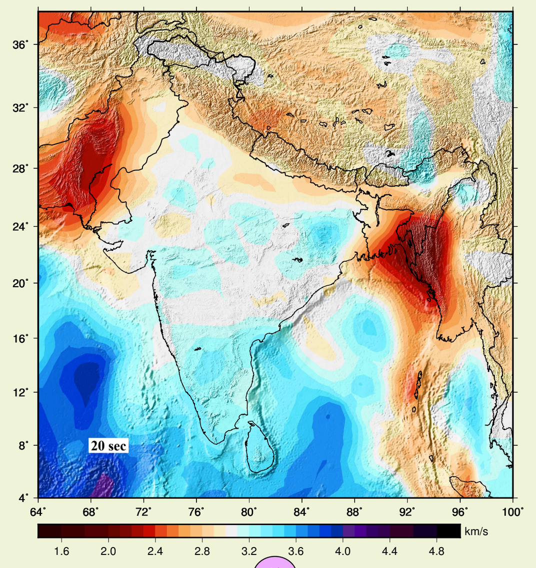

4b

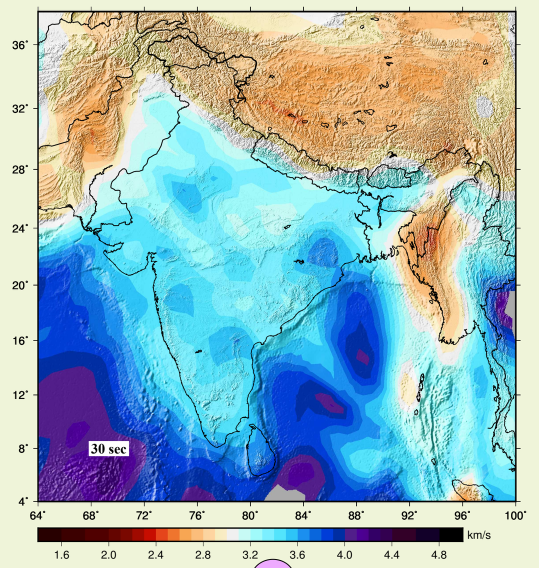

4c

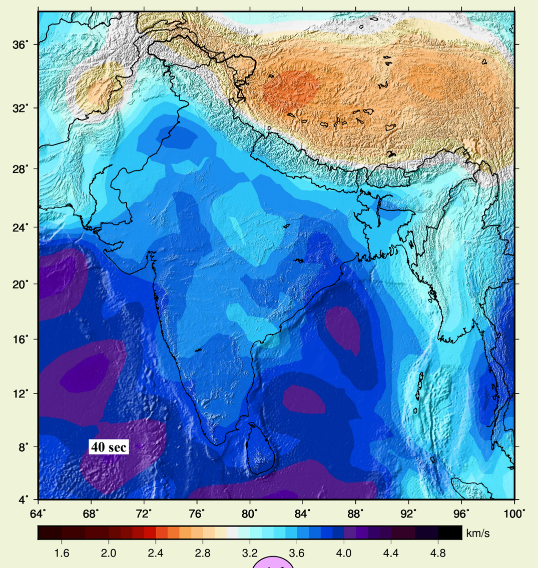

4d

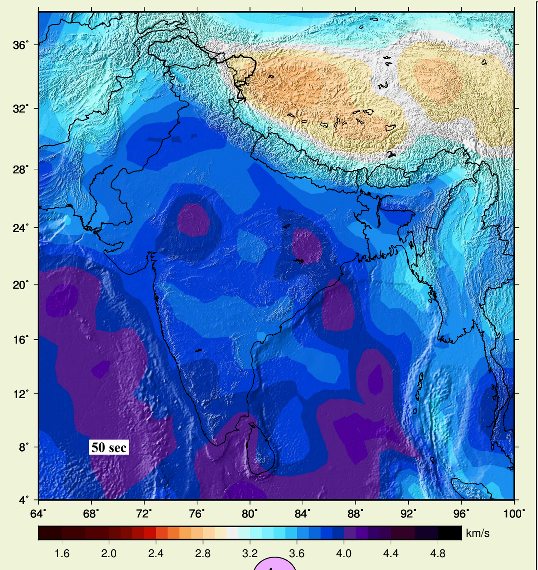

4e

A simplified geological setting showing major tectonic features of India and surrounding regions (taken from Maurya et al., 2016). Group velocity tomography maps at 20sec (figure 4b), 30sec (figure 4c), 40sec (figure 4d) and 50sec (figure 4e). Low periods tomography maps provide better constraints on the lateral velocity variations in the crust and consistently map the stable cratons, sedimentary basins and Himalayan fold and thrust belts. High velocity maps resolve the thicker crust beneath the Tibetan plateau and upper portions of the stable shield areas in the Peninsular India.

Isotropic inversion and Shear wave velocity profiles

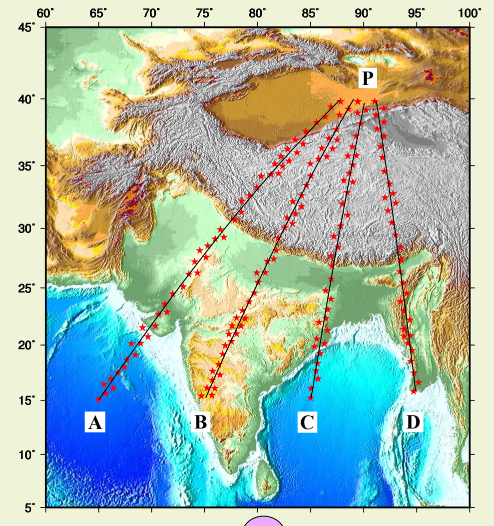

5a

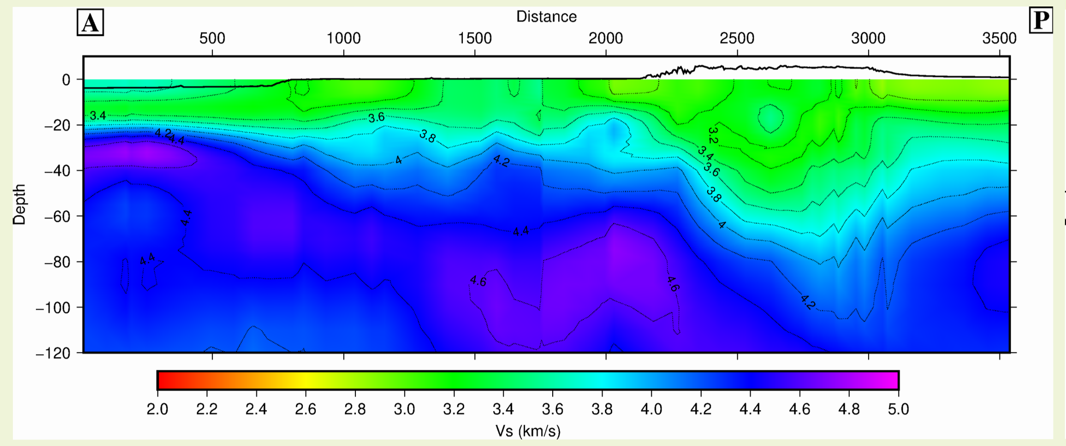

5b

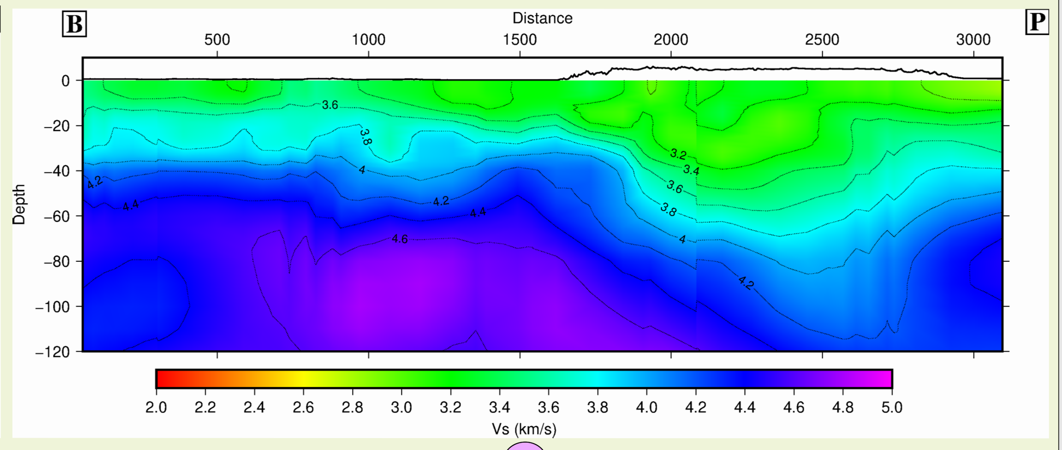

5c

Map (figure 5a) showing four profiles across the Himalayan arc across which the isotropic shear wave velocity profiles are shown in the figure 5b (AP), 5c (BP), 5d (CP) and 5e (DP). The red stars are the node points at which the slowness values were calculated and then projected on the black lines. Linear isotropic inversion of the tomography results were performed at each node using surf96, with the input model taken as layers of a)2km each from 0-40km depth, b)5km each from 40-80km depth and c)10km each from 80-120km depth.

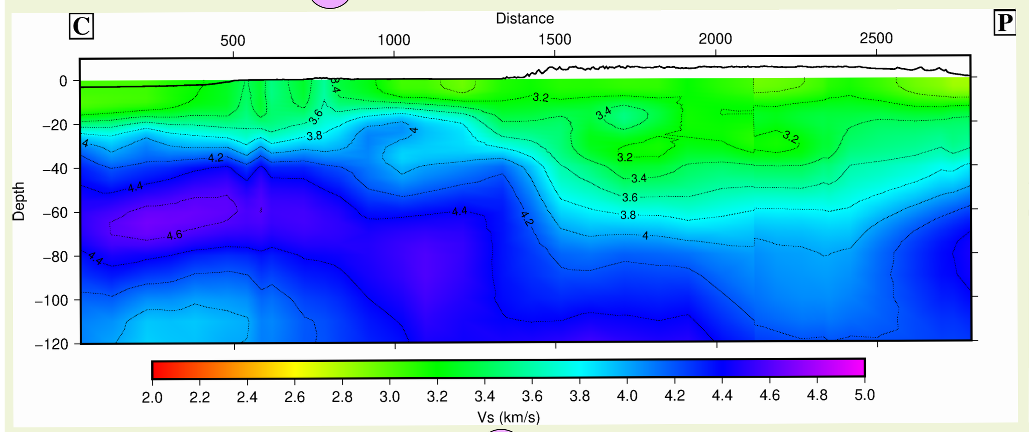

5d

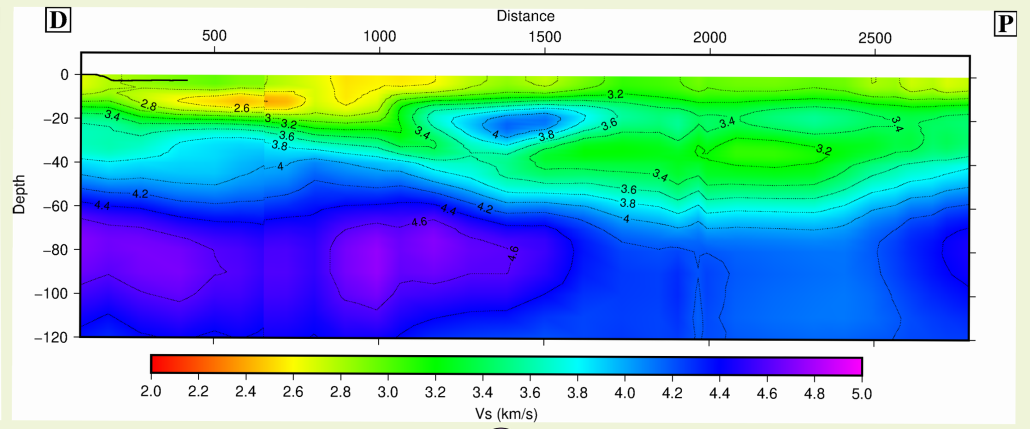

5e

Conclusions

1. Regions of Indian subcontinent are observed with better resolution (<4°) and lesser uncertainty (0.3km/s) in group velocity maps than previous studies.
2. Higher amount of raypaths aligned in a particular direction can lead to smearing and artifacts which can be compensated by comparable number of raypaths aligned in other directions as increase in intersection points will result in decrease in velocity biases.
3. Moho boundary is observed to be closely following ~4.1km/s contour in India-Tibet collision zone.

References

1. Acton et al.,2010 (JGR) doi:10.1029/2009JB007021, 2010.
2. Maurya et al., 2016 (JGR) doi:10.1002/2016JB012948, 2016.
3. Gilligan et al., 2018 (GJI) doi: 10.1093/gji/ggy172, 2018.

Acknowledgements

SD acknowledges IISER K fellowship, GMT v5.4.1, SAC v101.6a. SM acknowledges Academic Research Fund (ARF) from IISER Kolkata.